Antimicrobial wound dressings against fluorescent and methicillin-sensitive intracellular pathogenic bacteria

Sara Garcia-Salinas[†,‡,*], *Enrique Gámez-Herrera*[†], *Guillermo Landa*[†], *Manuel Arruebo*[†,‡], *Silvia Irusta*[†,‡,*], *Gracia Mendoza*[†,‡]

[†]Department of Chemical Engineering, Aragon Institute of Nanoscience (INA), University of Zaragoza, Campus Río Ebro-Edificio I+D, C/ Mariano Esquillor S/N, 50018 Zaragoza, Spain; and Aragon Health Research Institute (IIS Aragón), 50009 Zaragoza, Spain

[‡]Networking Research Center on Bioengineering, Biomaterials and Nanomedicine, CIBER-BBN, Madrid 28029, Spain

ABSTRACT

There is limited evidence indicating that drug-eluting dressings are clinically more effective than simple conventional dressings. To shed light on this concern, we have performed evidence-based research to evaluate the antimicrobial action of thymol (THY)-loaded antimicrobial dressings having antibiofilm forming ability able to eradicate intracellular and extracellular pathogenic bacteria. We have used four different *Staphylococcus aureus* strains, including the ATCC 25923 strain, the Newman strain (methicillin-sensitive strain, MSSA) expressing the coral green fluorescent protein (cGFP) from the vector pCN47, and two clinical reference strains, Newman-(MSSA) and USA300-(methicillin-resistant strain, MRSA), as traceable models of pathogenic bacteria commonly infecting skin and soft tissue. Compared to non-loaded dressings, THY-loaded polycaprolactone based electrospun dressings were also able to eliminate pathogenic bacteria in coculture models based on infected murine macrophages. In addition, by using confocal microscopy and the conventional microdilution plating method, we corroborated the successful ability of THY in preventing also biofilm formation. Herein, we demonstrated that the use of wound dressings loaded with the natural monoterpenoid phenol derivative THY are able to eliminate biofilm forming and intracellular *S. aureus* sensitive to methicillin more efficiently than their corresponding THY-free counterparts.

KEYWORDS: *electrospinning, polycaprolactone, essential oils, infection model, confocal microscopy, wound healing, thymol, Staphylococcus aureus*, methicillin-resistant *Staphylococcus aureus*

1. INTRODUCTION

In 1945, Sir Alexander Fleming claimed that the overuse of antibiotics leads to the evolution of resistance.[1,2] Different studies show that there is a direct relationship between antibiotic consumption and the diffusion of resistant bacterial strains.[3] Approximately, 80% of antibiotics sold in U.S.A. are administered to animals, which are lately ingested by humans.[2,4] Besides animal feeding, 30 to 60 % of antibiotics are also incorrectly prescribed, which leads to therapeutic complications and a potential increase of antibiotic resistance.[5] The economics in the search of new antibiotic molecules might not justify the necessary investment for the pharmaceutical industry.[6] In addition, despite all the global efforts to control and reduce the use and misuse of antibiotics, a retrospective report has recently demonstrated that the antibiotic use in 76 countries studied over 16 years (2000-2015) increased 65% (expressed as prescribed daily doses), and the antibiotic consumption rate increased 39%.[7] Thus, new alternatives have been developed to treat bacterial infections. For example, natural compounds and metal nanoparticles are proposed as antibiotic substitutes due to their multiple mechanisms of antimicrobial action.[8] The probability to develop bacterial resistance towards essential oils (EOs) is low. This fact may fall on the multicomponent nature and varied composition of EOs and in their ability to target multiple antibacterial pathways, meanwhile antibiotics normally focus on only one single target.[9] However, it has been reported that bacteria can modify its membrane composition and structure in response to subinhibitory concentrations of some antimicrobials present in EOs such as thymol (THY).[10] Therefore, sustained concentrations above minimal inhibitory concentrations should be maintained at all times to prevent resistances.

THY, a monoterpenoid phenol compound present in different EOs as that obtained from *Thymus vulgaris*, has demonstrated its antimicrobial activity against different bacterial strains such as *Staphylococcus aureus,* a major human pathogen which causes substantial morbidity and mortality in skin and soft tissue associated infections as well as in implant-associated infections.[11–13]

To overcome EOs solubility limitations and provide with sustained release, new pharmaceutical formulations have been proposed.[14] Nanotechnology has contributed to the development in different areas of medicine including diagnosis, therapy and in their combination (i.e., theragnostics).[15] Within the nanotechnology field, due to their large area per volume ratio, nanofibers outstand as ideal building blocks in different biomedical materials applied in drug delivery,[16] biomedical devices,[17] biosensing[18] or as dressings for wound healing.[19] Regarding this last application, the synthesis of polymeric electrospun nanofibers loading antimicrobial and anti-inflammatory drugs (including EOs), has been explored in the development of antimicrobial wound dressings.[20] In contrast to conventional fibers, nanofibrous patches contain fibers ranging from nanometers to micrometers showing high porosity, narrow diameter distribution and high-specific surface area prone to the release of loaded antimicrobial compounds. Some electrospun dressings are made of biomaterials recognized for their biocompatibility, biodegradability and lack of toxicity, such as natural or synthetic polymers (chitosan, collagen, polycaprolactone (PCL) or poly lactic-co-glycolic acid (PLGA)).[21] PCL is a biocompatible polymer approved by the FDA in many devices due to its high biocompatibility and controlled hydrolytic biodegradation.[22] Loaded with antimicrobial drugs, PCL nanofibers have demonstrated high efficiency not only preventing infection development, but also avoiding biofilm formation.[23–25]

Biofilms are populations of microorganisms aggregated and embedded in an organic self-secreted extracellular matrix made of polysaccharides (EPS) which provides bacteria with a protective environment to medical treatments. It is well known that bacteria on chronic infected wounds do not remain in their free-living planktonic state but organized as biofilms.[26] Within the biofilm, there are intercellular signaling molecules produced by bacteria that respond to cell population density by gene regulation. In response to factors secreted by other bacteria in the community, bacteria can coordinate their activities, control the biofilm growth pattern or change their phenotype and thus, their virulence factors.[27] Antibiotics can penetrate the extracellular surface of planktonic bacteria, but bacteria within the biofilm can be protected and the antibiotic diffusion impaired.[28] Against this fact, EOs have been studied for their biofilm disruption potential. It has been reported the ability of some EOs to inhibit biofilm formation or disrupt already formed biofilms, suggesting their potential use in food preservation and in antimicrobial therapies.[29,30] Their antibiofilm activity may be attributed to different mechanisms: the inhibition of bacterial adhesion to surfaces at an initial stage, or the inhibition of Quorum Sensing (cell to cell communication).[30] THY has been shown as an effective compound to inhibit biofilm formation, not only in monomicrobial cultures of *S. aureus*, but also in polymicrobial cultures of different bacteria (e.g., *S. aureus, Listeria monocytogenes*).[12,29] This effect may be attributed to the disruption of bacteria membrane permeability and thus, hindering surface adhesion.[31] Therefore, THY reduces bacterial growth, interferes with biofilm formation and promotes biofilm eradication.[32]

Exposed subcutaneous tissues have been shown as critical scenarios for potential infection development facilitating a suitable microenvironment for bacteria colonization and contamination.[33] The risk of infection represents a general concern in skin and soft tissue

open wounds, where each phase of wound healing is challenged by the possibility of microbial infection.[34,35] Following postsurgical wound analysis, it has been demonstrated that the average hospitalization period rises from 14 to 24 days when wounds become infected.[36] Infected wounds are characterized by a failure in the inflammation, re-epithelialization and remodeling phases. The most representative signs of infection are pain, erythema, edema, heat and purulence, exudate, discoloration or wound breakdown.[37]

For a successful tissue regeneration, the wound healing process requires the complete removal of any microbial exogenous contamination. Macrophages play an essential role in wound healing, not only eliminating pathogens or dead cells, but also releasing cytokines, growth and angiogenic factors that take part in the wound healing process.[38] In this regard, tissue-resident macrophages recognize pathogen-associated patterns, such as the presence of bacterial endotoxin lipopolysachharide (LPS) during infection, recruiting other cells which help fighting a potential infection.[39] *S. aureus* is a pathogen described to survive within phagocytic cells, such as macrophages, persisting in parts of its life-cycle intracellularly during infections.[13,40,41] Co-culture models of *S. aureus* infected macrophages have been developed to study the behavior of bacteria under the presence of different antimicrobial treatments.[41–43]

Herein, we have developed electrospun THY-loaded PCL nanofibers and we have studied the effect of these advanced drug-eluting wound dressings against different *S. aureus* strains: ATCC 25923 strain, GFP-expressing antibiotic sensitive *S. aureus* (MSSA) growth, and two clinical reference strains, Newman-(MSSA) and USA300-(methicillin-resistant strain, MRSA). Three different infection models have been developed: (a) planktonic bacteria, (b) biofilm formation and (c) a co-culture model of J774 macrophages infected with GFP-expressing *S. aureus*. Besides the development of quantitative methods, confocal microscopy

was used to observe both biofilm formation and bacteria eradication in the co-culture model after treatment with different dressings based on THY-loaded PCL nanofibers.

2. EXPERIMENTAL SECTION

2.1. Materials

PCL (*Mn* = 80,000 Da), (*S*)-(-)-limonene (food grade, ≥95%), naproxen sodium salt (98–102%), phosphate buffered saline (PBS), thymol (THY, >98.5%), Erythromycin, Bovine Serum Albumin (BSA), Calcofluor White stain and CellCrown™ inserts (24-well plate inserts) were purchased from Sigma-Aldrich (Germany). Dichloromethane (DCM, >99%), *N*,*N*-dimethylformamide (DMF, >99%), Phalloidin 546 and DAPI were obtained from Fisher Scientific (USA). Tryptone soy broth (TSB) and tryptone soy agar (TSA) were purchased from Laboratorios Conda-Pronadisa S.A. (Spain). *S. aureus* ATCC 25923 strain was obtained from Ielab (Spain), while GFP-expressing antibiotic sensitive *S. aureus* (MSSA) and the two clinical strains Newman-(MSSA) and USA300-(MRSA) were kindly donated by Dr. Cristina Prat, Institut d'Investigació en Ciències de la Salut Germans Trias i Pujol (IGTP, Spain). Paraformaldehyde (PFA) 4% in PBS was acquired from Alfa Aesar (Germany). Saponin from Quillaja Bark pure and SDS for molecular biology were purchased from AppliChem (Germany). Fetal Bovine Serum (FBS) was obtained from Gibco (UK) while penicillin-streptomycin-amphotericin B (PSA) was purchased from Biowest (France) and Dimethyl sulfoxide (DMSO) from Merck Millipore (Germany). MTT (3-(4,5-dimethylthiazol-2-yl)-2,5-diphenyltetrazolium bromide) was obtained from Invitrogen (USA).

2.2. Preparation of PCL and THY-loaded PCL nanofibers

A solution of PCL (10 w/w %) was prepared in dichloromethane (DCM) and dimethylformamide (DMF) at 1:1 volume ratio. For the preparation of THY-loaded PCL nanofibers, THY was added to the polymeric solution at 20 w/w % concentration (referred to the PCL mass). The mixture was stirred for 30 min before electrospinning.

An Yflow 2.2 D500 electrospinner equipped with a rotating drum collector (100 rpm) was used to obtain bare and THY-loaded PCL-nanofibers. The collection drum was covered with aluminum foil to facilitate the recovery of the electrospun nanofibers. PCL and PCL-THY solutions were electrospun through a 22-gauge needle with a syringe pump working at 1.0 mL/h flow rate. The distance from the tip of the needle to the collector was 18 cm. The voltage applied to the collector plate was -7 kV and the voltage applied to the needle was +10 kV with the aim of obtaining a stable Taylor cone. Homogeneous patches of bare and THY-loaded PCL nanofibers were obtained after 8h of electrospinning.

2.3. Physico-chemical characterization of the electrospun nanofibers

The resulting electrospun patches were observed by scanning electron microscopy (SEM) using an Inspect F50 SEM microscope. Samples were covered with an Au/Pd layer before electronic visualization. Resulting images were analyzed and nanofiber sizes measured (N = 100) using the ImageJ software (Version 1.48f, NIH, USA).

THY loading in the fibers was determined by GC-MS using a Shimadzu 2010SE GC-MS chromatograph equipped with an AOC 20i injector and a Zebron ZB-50 capillary column (30 m x 0.25 mm, 0.25 μm thickness, Phenomenex). Ten mg of nanofibers were dissolved in DCM:acetonitrile (1:1), each sample was diluted with known amounts of methanol and 5 ppm of (*S*)-(-)-limonene that was added as internal standard. Helium was used as carrier gas. Drug loading (DL) was calculated using Eq.1:

$$DL\ (\%) = \frac{We}{Wn}\ x\ 100$$

Encapsulation efficiency (EE) was calculated following Eq. 2:

$$EE\ (\%) = \frac{We}{Wt}\ x\ 100$$

Being W_t the theoretical THY load added, W_e the measured THY load chromatographically quantified and W_n the total weight of the THY-loaded nanofibers.

2.4. Release of THY

THY release was carried out under temperature-controlled conditions using an IKA® KS 130 orbital shaker. Ten mg of PCL-THY patches were immersed in 4 mL of PBS and kept at 37 ºC under stirring (150 rpm). At different time points up to 24h, the supernatant from independent samples at each time was collected and analyzed in an Acquity UPLC® Waters liquid chromatography system and Waters® Empower™ chromatographic software (Waters, USA). An Acquity UPLC® Waters BEH C18 column (2.1 x 50 mm, 1.7 µm particle diameter) was employed for the analysis of THY. In the determination, 25 ppm of naproxen was included as internal standard.

The release kinetics were determined by fitting the data through the Peppas-Sahlin model. The correlation coefficient (R^2) value was calculated from the linear regression of these plots following this equation (Eq. 3):

$$\frac{M_t}{M_T} = K_1 t^N + K_2 t^{2N}$$

where M_t/M_T is the drug release fraction at time t, K_1 and K_2 are constants and N is the diffusional exponent.

2.5. Viscosity and conductivity measures

Relative viscosity of precursor solutions was measured at 25 ºC using a Visco Basic Plus viscosimeter (Visco Basic, Spain). Solutions conductivity was measured with a multimeter MM41-Criston (Hach Lange, USA).

2.6. Bactericidal activity

Antibacterial activity was determined in a methicillin-sensitive *S. aureus* Newman strain expressing the coral green fluorescent protein (cGFP) from the vector pCN47. Minimal inhibitory (MIC) and bactericidal (MBC) concentrations were tested following the standard microdilution method.[44] Different concentrations of free THY (0.01-0.15 mg/mL) were analyzed in liquid growth medium (TSB) and THY-loaded PCL nanofibers were studied in agar broth (TSA) according to the ASTM E-2180-18 standard test method.[45] A positive control (untreated bacteria) was also included in both methods.

To assess inhibitory and bactericidal effects of free THY on cGFP expressing *S. aureus* cultures, a 20 mg/mL stock solution of THY in DMSO and diluted in TSB up to reach study concentrations was prepared. A solution of 10^5 Colony Forming Units (CFU)/mL of bacteria was added to different free THY concentrations and incubated for 24h at 37 ºC under shaking (150 rpm). After this time, bacterial suspensions were diluted in PBS and plated on TSA to count colonies after 24h of incubation at 37 ºC.

Separately, patches composed of THY loaded nanofibers were cut, weighted and sterilized using UV light (30 min each side). Warm TSA (47 ºC) was inoculated with 10^5 CFU/mL of cGFP expressing *S. aureus*. Nanofiber-based patches were placed in 12-well plates and 3 mL of inoculated TSA were added to each well. Samples were incubated at 37 ºC for 24h in a closed box with water to keep an adequate humidity. After incubation, each sample was collected with 7 mL of TSB, sonicated and vortexed for 1 min. Bacterial suspensions were diluted in PBS and plated on TSA to count colonies after 24h of incubation at 37 ºC.

2.7. Antibiofilm activity

Four *S. aureus* strains (ATCC 25923, GFP-expressing antibiotic sensitive *S. aureus* (MSSA) growth, and the two clinical reference strains Newman-(MSSA) and USA300-(MRSA) were overnight cultured until reaching stationary phase. To evaluate the effect of PCL-THY against biofilm formation, two different procedures with varied PCL-THY masses and incubation times were carried out in µ-dish 35 mm ibiTreat plates:

- In the first methodology, 10^4 CFU/mL of bacteria were put in contact with 5 and 7 mg of PCL-THY patches and incubated for 24h at 37 ºC.
- In the second approach, bacteria in the exponential growth phase (10^4 CFU/mL) were separately prepared and 10 and 12 mg of PCL-THY patches were added to the culture and incubated for 1h. Later, patches were removed, and culture media was kept at 37 ºC for 24h.

These parameters were chosen as a result of the bactericidal effects and cell viability percentages obtained in order to use PCL-THY amounts able to eradicate bacteria but harmless to eukaryotic cells.

After incubation, both approaches were processed simultaneously. Planktonic cells were removed, and wells were washed twice with PBS. Biofilm formation was analyzed by following two different methods in which THY-free patches (composed of just PCL) were tested as controls:

- For confocal microscopy, the biofilm matrix was treated for 1 min with Calcofluor White stain and washed with PBS. Next, 2 mL of PFA 4% in PBS were added to each plate. After 30 min incubation, samples were mounted in Mowiol mounting medium (Thermo Fisher Scientific, USA) to be further visualized by confocal microscopy (Confocal Zeiss LSM 880 with Airyscan).

- For bacteria quantification, biofilm in PBS was sonicated for 15 min in an ultrasonic water bath to ensure its detachment from the bottom of the wells. Later, detached bacteria concentrations were tested following the conventional microdilution method[44] to be then plated on TSA and colonies counted after incubation (24h, 37 ºC).

2.8. Cell culture and cytotoxicity assays

J774 macrophages were used to evaluate the cytotoxic effects of THY-loaded patches prior to their application in a co-culture model with GFP-expressing *S. aureus*. Macrophages were grown in high-glucose DMEM supplemented with 10% FBS and 1% PSA and incubated in a humidified atmosphere at 37 ºC and 5% CO_2.

Different amounts of PCL-THY were tested at different time points:

- First, cells were seeded in 6-well plates (48000 cells/cm^2), and 5 and 7 mg of PCL-THY were added to the cultures (2 mL). Samples were incubated at 37 ºC, 5% CO_2 for 24h. Later, patches were removed, and cells were washed twice with PBS.
- Another approach was followed using 10 and 12 mg of PCL-THY which were added to 2 mL of cell cultures (48000 cells/cm^2) and incubated for 1h (37 ºC, 5% CO_2). Later, these patches were removed, and cells were further incubated with supplemented DMEM at 37 ºC, 5% CO_2 for 24h. Then, cells were washed twice with PBS.

After cell treatment with the loaded patches following both approaches, the MTT cytotoxicity assay for assessing cell metabolic activity was used by preparing a stock solution of the tetrazolium dye at 5 mg/mL in PBS. Cells were incubated with 0.5 mg/ mL of the MTT dye for 3h at 37 ºC. After the incubation period, medium was removed, and the dye was solubilized with a solution containing DMSO (99.4% v/v), SDS (0.1% w/v) and acetic acid

(0.6% v/v) for 15 min. The dye is reduced forming an insoluble formazan salt when the metabolism of cells is active. This salt was dissolved to obtain a purple solution which was quantified at OD of 540 nm (Multimode Synergy HT Microplate Reader; Biotek, USA). Viability percentages were calculated dividing the OD of treated samples by the OD obtained from the positive control samples. Mean ± SD of three replicas are represented.

2.9. *In vitro* model of infection of J774 macrophages

J774 macrophages were seeded in µ-dish 35mm ibiTreat plates (130000 cells/cm^2) overnight. Prior to the infection assays, supplemented DMEM containing antibiotics was removed, cells were washed twice with PBS and DMEM renewed without adding antibiotics in order to avoid hampering infection. Non-infected and infected cells without treatment were also run as control samples (data not shown). Equally, THY-free patches (PCL) were tested in the cultures to evaluate the treatment effect. Both methodologies described in the cell cytotoxicity section were followed according to the corresponding patches weight and the results obtained in the cytotoxicity assays to elucidate the efficiency of the patches related to their weight and thus, their THY loading. Patches were added to culture cells and then infected with 10^5 CFU/mL of GFP-expressing *S. aureus* in DMEM without antibiotics previously prepared. Treated cultures were incubated for 30 min (10 and 12 mg PCL-THY) or 24h (5-7 mg PCL-THY) at 37 ºC and 5% CO_2. After those time periods, patches were removed, cells were washed twice with PBS and fixed in PFA 4% during 30 min at room temperature.

Confocal microscopy was then used to monitor the effect of PCL-THY in the infection model of J774 macrophages by GFP-expressing *S. aureus*. After fixation, cells were first washed with PBS-BSA 1% and secondly, with saponin 0.1% in PBS-BSA solution. Straightaway, the plates were incubated in the dark with 500 µL of phalloidin 546 (1:200 in PBS-BSA-

saponin prepared solution; Thermo Fisher Scientific, USA) for 1h at room temperature. After incubation, cells were rinsed with PBS-BSA 1% and then with distilled water. Finally, coverslips were mounted on glass slides in DAPI-Mowiol mounting medium (Thermo Fisher Scientific, USA). Samples were analyzed under confocal microscopy (Confocal Zeiss LSM 880 with Airyscan). Z-stack orthogonal projections were used to visualize the presence of bacteria inside the eukaryotic cells.

2.10. Statistical analyses

All values are reported as Mean ± SD. Statistical analysis of data was performed using Prism 7 software (Version 7.04, GraphPad Software Inc., US). Three replicas for each biological experiment were performed. A one-way analysis of variance (ANOVA) set for multiple comparisons with a Dunnett's post-test was used. Statistically significant differences were considered when $p \leq 0.05$.

3. RESULTS AND DISCUSSION

3.1. Physico-chemical characterization of the electrospun nanofibers

Figure 1 shows SEM micrographs of PCL and THY-loaded PCL nanofibers. Both fibrous patches were homogeneous in their fiber diameter distribution having a bead-free surface. PCL patches showed mean fiber diameters of 779 ± 86 nm, meanwhile THY-loaded PCL nanofibers mean diameter was 794 ± 96 nm. Sadeghianmaryan et al.[46] also obtained PCL nanofibers with a small dispersity in size and random orientation following the same methodology.

The morphology and dimensions of the electrospun fibers depend on processing and polymer solution parameters.[47] Synthesis parameters were the same for PCL and PCL-THY patches, using a polymer flow rate of 1 mL/h and a distance from the tip to the collector of 18 cm.

The presence of THY in the synthesis solution did not change the ionic conductivity (22.2 μS for PCL and 20.8 μS for PCL-THY) and, despite of the increase in the solution viscosity (from 1.4 to 1.6 cP for PCL and for PCL-THY, respectively), it did not affect the resulting fibers morphology.[47] In our case, the increase on the resulting fibers diameters compared to our previous results using similar experimental conditions[19] would be related to the use of a rotating drum collector instead of a flat collector. Alfaro De Prá et al. also demonstrated that thicker PCL fibers with average diameters of 663 ± 334 nm can be obtained using a rotatory drum collector instead of a flat one.[48] THY loading in the prepared fibers was 8.2 ± 0.9 wt.% which renders an encapsulation efficiency of 40.8 ± 4.6 wt.%. This low EE achieved could also be related to the use of a rotating collector, since for carvacrol (isomer of THY) loaded polyvinyl acetate fibers prepared using this collection system, the EE was also low (43-55 %) attributed to the evaporation of the monoterpenoid phenol derivative.[49] The study of release kinetics demonstrated a fast THY release from the PCL-THY patches. Figure 1E shows that 30% of the encapsulated THY was released in the first hour. Peppas and Sahlin release kinetics model (Eq. 3) was the best mathematical fit for THY release showing a R^2 correlation coefficient of 0.993 (Figure 1E). This model describes a drug release occurring through the coupling of Fickian diffusion and polymer chains relaxation phenomena[50]. In our case the $K_1 >> K_2$ implies that the Fickian diffusion is the predominant mechanism in the THY release.

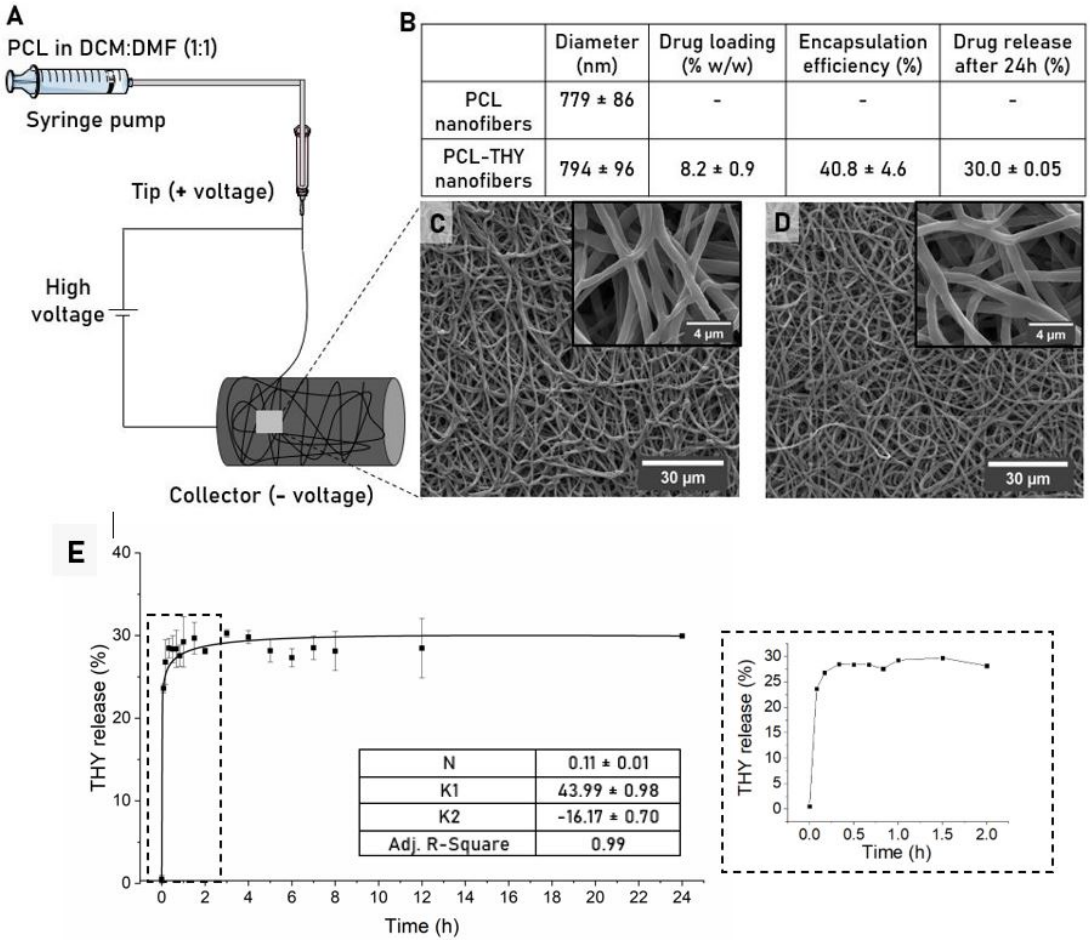

	Diameter (nm)	Drug loading (% w/w)	Encapsulation efficiency (%)	Drug release after 24h (%)
PCL nanofibers	779 ± 86	-	-	-
PCL-THY nanofibers	794 ± 96	8.2 ± 0.9	40.8 ± 4.6	30.0 ± 0.05

Figure 1. Patches synthesis and characterization. (A) Scheme depicting the PCL nanofibers synthesis by electrospinning. (B) Table shows nanofiber diameters and PCL-THY drug loading (w/w %) and encapsulation efficiency (%). Mean ± SD (N=100). (C) PCL morphological characterization by SEM. (D) PCL-THY morphological characterization by SEM. (E) THY release and Peppas and Sahlin fitting parameters.

3.2. Bactericidal activity

Figure 2 shows the antibacterial activity of free and THY encapsulated PCL determined in cultures of GFP-expressing *S. aureus*. 0.05 mg/mL of free THY were enough to significantly inhibit bacteria growth, showing a reduction from 10^9 to 10^7 CFU/mL. When bacteria were

310 treated with 0.15 mg/mL of free THY, no growth was found, meaning that the MBC was
311 reached.
312 When bacteria were treated with PCL-THY, it was observed that 10 mg of PCL-THY reached
313 the MIC inhibiting bacteria growth from 10^9 to 10^6 CFU/mL, whereas 12 mg of PCL-THY
314 were enough to avoid GFP expressing-*S. aureus* growth (MBC) in an agar culture of 3 mL
315 of volume containing an inoculum of 10^5 CFU. Considering THY loading and release
316 kinetics from the patches, a mat of 10 mg would provide a THY concentration released of
317 0.08 mg/mL in the analyzed time whereas 12 mg of PCL-THY would release THY to the
318 medium reaching a THY concentration of 0.1 mg/mL. The slight MIC and MBC differences
319 observed between free THY and THY released from the PCL-THY patches can be associated
320 with the experimental method followed, since free THY is challenged against bacteria in a
321 liquid culture medium (TSB), whereas THY-loaded patches were studied using solid agar
322 (TSA).
323 Wound healing may be impaired by wound infection mediated by different bacteria. The
324 microorganisms closely related to the colonization of skin and soft tissue wounds are
325 generally from the *Staphylococci* family (in particular, *S. epidermidis* and *S. aureus).*[28] In
326 previous studies, we have demonstrated that THY is one of the best natural compounds
327 inhibiting bactericidal growth of *S. aureus* strains. Free THY showed a MIC of 0.2 mg/mL
328 and a MBC of 0.3 mg/mL against a *S. aureus* ATCC 25923 strain.[12] In the treatment with
329 THY, Badawy et al.[51] reported a MIC for ATCC 6538 *S. aureus* of 0.13 mg/mL, meanwhile
330 Rua et al.[52] identified a MIC in the range of 0.46-0.51 mg/mL for different *S. aureus* strains.
331 These previous studies point to the higher sensitivity of the GFP-expressing *S. aureus* strain
332 used in this work since a concentration of 0.05 mg/mL of free THY was enough to inhibit
333 the bacteria growth (MIC), whereas the complete elimination of the bacteria was reached

when free THY concentration was 0.15 mg/mL. Moreover, higher sensitivity of this strain was also found for THY loaded PCL fibers. The comparison of these results with our previous studies[19] showed the same pattern. In the current study, 12 mg of THY-loaded PCL patches (corresponding with 0.1 mg/mL of THY released in 24h) were enough to achieve the MBC when working with GFP-expressing *S. aureus*, meanwhile 30 mg of PCL-THY (0.38 mg/mL of THY released in 24h) were needed to completely eradicate bacteria using the *S. aureus* ATCC 25923 strain.[19] These differences in THY susceptibility may be attributed to phenotypic differences among *S. aureus* strains as explained above.

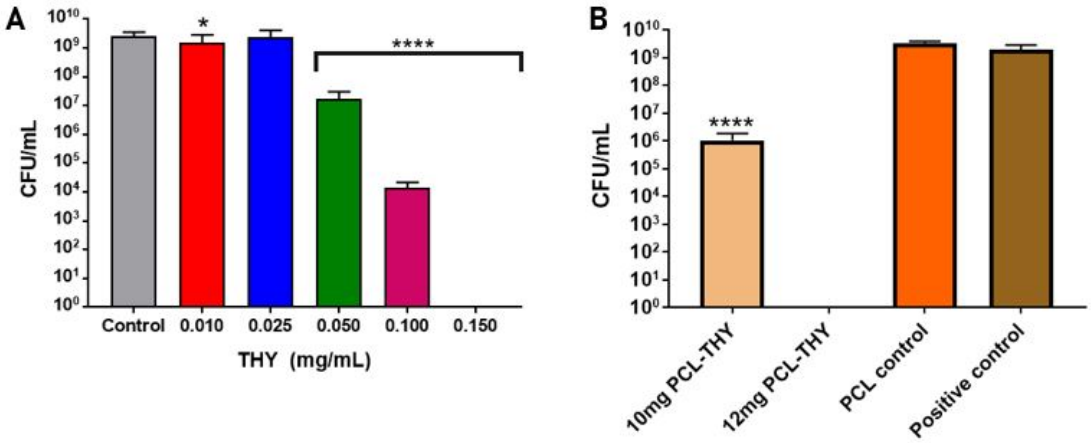

Figure 2. Effect of THY treatment in GFP-expressing *S. aureus* growth (CFU/mL) in contact for 24h. (A) Free THY (0.01-0.15 mg/mL). (B) PCL-THY (10-12 mg). All samples are statistically compared with the positive control sample (non-treated bacteria). *p<0.05; ****p<0.0001. Mean ± SD of three replicas are represented.

3.3. Antibiofilm activity

GFP expressing-*S. aureus* biofilm formation was monitored by confocal microscopy by using the Calcofluor White stain (Figure 3). As mentioned in the experimental section, two approaches were followed based on the incubation times and the amount of THY-loaded PCL

patches used regarding the bactericidal effects and cell viability percentages obtained in order to use PCL-THY amounts able to eradicate bacteria but harmless to eukaryotic cells.

As it can be observed in Figure 3, THY-free PCL (7 and 12 mg; left images) patches let bacteria (stained in green) grow all over the well, forming a homogeneous layer of biofilm, which was clearly stained with Calcofluor White (in blue) on top of the bacteria settled underneath (green layer), as depicted in the bottom panels of both images. These results suggest that bacteria released the polymeric extracellular material typical of biofilm on the wells. However, the loaded patches clearly decreased the amount of bacteria present in the wells showing lower bacteria density when the patch´s weight was increased. Right images clearly show that the presence of bacteria was almost totally eliminated when the THY concentration was increased. In this case, although all treated samples were stained with Calcofluor White, none of them showed a top coating labelled in blue which would be characteristic of biofilm formation, demonstrating the lack of biofilm formation and highlighting the ability of the loaded patches to avoid or eradicate biofilms.

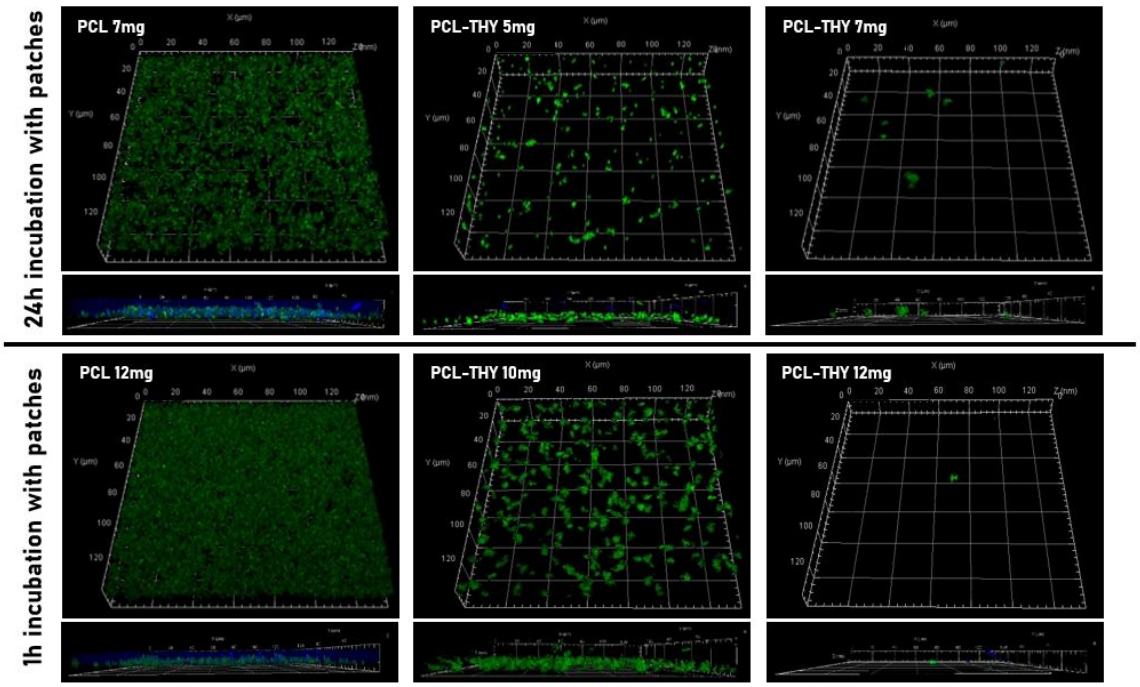

Figure 3. Confocal laser scanning microscopy was performed to evaluate the effect of different THY-loaded patches having different weights (5-7 mg and 10-12 mg) and different incubation times (1h and 24h), regarding the bactericidal effects and cell viability percentages obtained, compared with PCL control samples. For each incubation time, the three upper images correspond to GFP-expressing *S. aureus* attached to the bottom of the well. Bottom images show the Calcofluor stain of biofilm formed. Bacteria are depicted in green whereas biofilm stains in blue.

These qualitative results were confirmed with a quantitative method in which not only the GFP-expressing antibiotic sensitive *S. aureus* (MSSA) was assayed, but also other three strains were analyzed to corroborate the bactericidal potential of the synthesized mats: ATCC 25923, and the two clinical reference strains Newman-(MSSA) and USA300-(MRSA).

Attached bacteria were collected from the bottom of the wells and cultured in agar plates. Figure 4 shows the bacteria growth quantification after treatment following both methodologies. Positive controls (7-30 mg of PCL patches) reached 10^9 CFU/mL of bacteria growth in 24h whereas the treatment with 5-7 mg of PCL-THY for 24h (Figure 4A) or with 10-12 mg of PCL-THY for 1h (Figure 4B) displayed a significant decrease in bacterial growth in the range of 10^5-10^6 CFU/mL, confirming the qualitative results showed in Figure 3. *S. aureus* ATCC 25923 (Figure 4C) exerted a significant inhibition of bacteria growth (10^7 CFU/mL) when biofilm was treated with 10 mg of PCL-THY while the addition of 30 mg of the mat were able to completely eliminate the biofilm. On the other hand, the clinical isolates Newman-MSSA (Figure 4D) and USA300-MRSA (Figure 4E) showed a significant decrease in bacteria proliferation at the highest mat weight assayed (30 mg) achieving bacteria growth of 10^4 and 10^8 CFU/mL, respectively, (whereas for the THY-free mats bacteria grew until reaching ~10^{10} CFU/mL), which are in accordance with their sensitive and resistant characteristics.

Considering the release kinetics results, 5 and 7 mg of PCL-THY patches would release in 24h 0.06 and 0.09 mg/mL of THY, respectively. These concentrations in which we obtained MIC values, correlate with the inhibitory concentrations when using free THY against planktonic bacteria. Those results highlight the potential of these patches to provide with prophylaxis against biofilm formation and to reduce already formed biofilms.

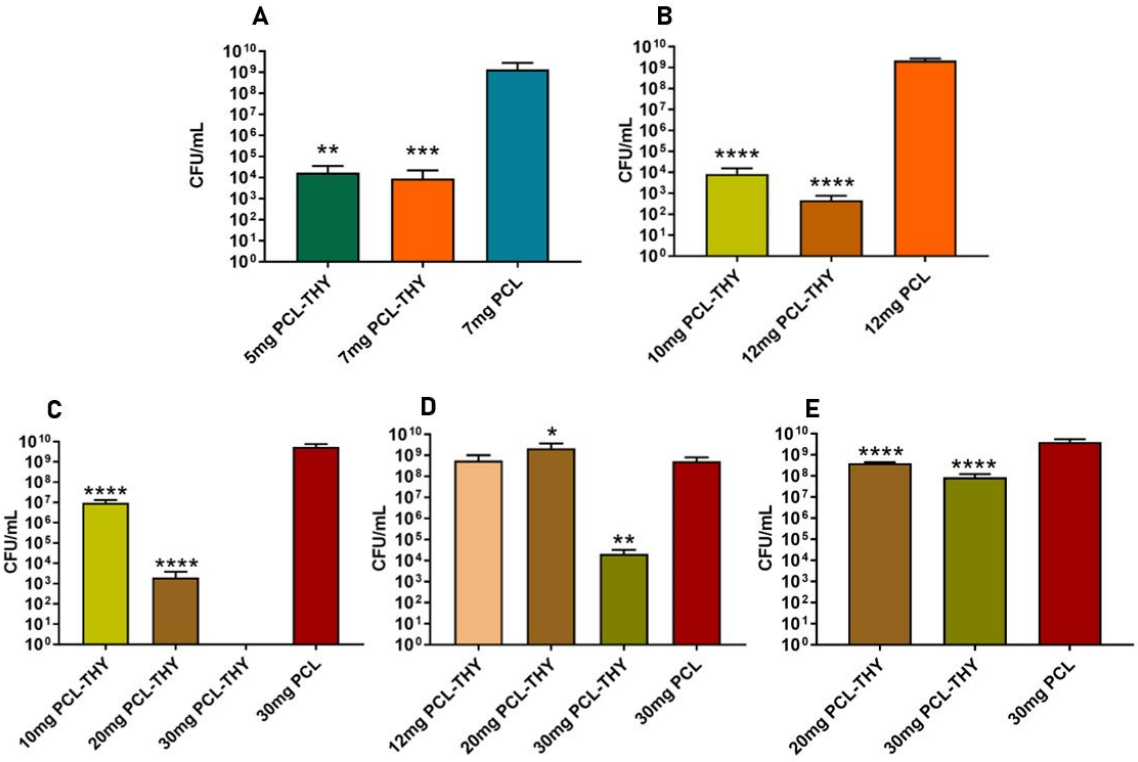

Figure 4: Quantification of GFP-expressing *S. aureus* (Fig. 4A and 4B), *S. aureus* ATCC 25923 (Fig. 4C), *S. aureus* Newman (MSSA clinical strain; Fig. 4D) and *S. aureus* USA300 (MRSA clinical strain; Fig. 4E) to evaluate biofilm formation against different treatments with PCL-THY: (A) 5-7 mg for 24h; (B) 10-12 mg for 1h, (C, D and E), 10-30 mg PCL-THY for 24h. Different THY-loaded patches of different weights (5-30 mg) and different incubation times (1h and 24h) were selected regarding the bactericidal effects and cell viability percentages obtained. Results derived from PCL-THY are statistically compared to those obtained from the THY-free PCL patches used as control. **p<0.01; ***p<0.001; ****p<0.0001. Mean ± SD of three replicas are represented.

A recent study states that 78% of non-healing chronic wounds contain biofilms.[34] The elimination of bacterial bioburden is essential to promote wound healing in chronic wounds.[53] Sharifi *et al.* demonstrated that sub-MIC concentrations (MIC/2 to MIC/16) of different EOs obtained from *Thymus daenensis* and *Satureja hortensis* in contact with *S. aureus* for 24h, significantly prevented biofilm formation.[31] In this sense, Yuan et al. also showed the efficiency of free THY in the inhibition of biofilm obtained from the non-clinical MRSA strain TCH1516 (ATCC BAA-1717). Biofilm formation and mature biofilm were inhibited by the treatment with up to 512 µg/mL of free THY, a concentration much higher than those released from our mats, though not achieving the complete eradication of bacteria growth.[54] Moreover, Cabarkapa *et al.* treated bacteria (*Salmonella* Enteriditis) with sub-MIC (MIC/2-MIC/4) concentrations of *Origanum* and *Thymus* essential oils as well as their active components carvacrol and THY, and results showed that biofilm formation was inhibited.[32] These studies corroborate our results, not only 7 mg of PCL-THY eliminate already formed biofilms, but also we demonstrate that the exposition to 5 mg PCL-THY for 24h, reduces bacterial attachment to the well. The obtained results may evidence that cell wall damage can negatively affect bacterial attachment as we previously described[12], which, according to Kerekes et al.[29] represents the first step in biofilm formation, followed by formation of microcolonies, maturation and cell dispersal.[29,31,55] The effect of THY against bacterial adhesion has also been demonstrated by Yuan et al.[54] when they analyzed PIA (Polysaccharide Intracellular Adhesion), a component involved in adhesion and aggregation. This component was reduced under the presence of THY and thus, bacteria could adhere to materials at the initial stage, but they were unable to form biofilms due to a reduced cell-to-cell adhesion.[54,56] Therefore, THY reduces bacterial growth, interferes with biofilm formation and promotes biofilm eradication.[32]

3.4. Cytotoxicity assessment of PCL-THY patches

Cytotoxicity of PCL-THY was studied in J774 macrophages at cell metabolism level using the MTT reduction assay. This method depends on the cellular activity of viable cells by producing a colored solution. Cells were exposed to different amounts of PCL-THY following the two methodologies described in the experimental section. The results obtained from both approaches were compared with cells treated with THY-free PCL patches (control samples).

In the first approach, cells were treated with 5 and 7 mg of PCL-THY for 24h. As depicted in Figure 5, a 50% cell growth inhibition was attained with 7 mg of PCL-THY, which corresponds to 0.09 mg/mL of THY released. However, the treatment with 5 mg of PCL-THY (0.06 mg/mL of THY released in 24h) displayed a 80% cell viability after 24h incubation, classifying the material as non-cytotoxic (according to the value established by the ISO 10993-5).[57]

Considering the direct relationship among increased concentration and cell toxicity, the treatment with more than 7 mg of PCL-THY for 24h would reduced significantly cell viability at levels below 70%. Due to that fact and keeping in mind that inhibitory and bactericidal concentrations were achieved with 10 and 12 mg PCL-THY, cells were treated with 10 and 12 mg PCL-THY but for a reduced incubation time (just 1h). Following this protocol, cell viability was quite similar for the mats weights evaluated, obtaining >70% of viability required to consider these concentrations as non-cytotoxic, which corresponds to 0.12 mg/mL using 10 mg PCL-THY and 0.14 mg/mL using 12 mg PCL-THY for 1h.

The cytotoxicity caused by THY against eukaryotic cells is related to its non-selective antiseptic character. During the regenerative process in an infected wound after adding an antiseptic, pathogenic prokaryotic cells are removed but also some somatic eukaryotic ones.

However, due to the immune response, new regenerative cells are recruited to the wounded area compensating the initial loss owing to the antiseptic effect. In addition, short contact times would minimize this cytotoxic effect.

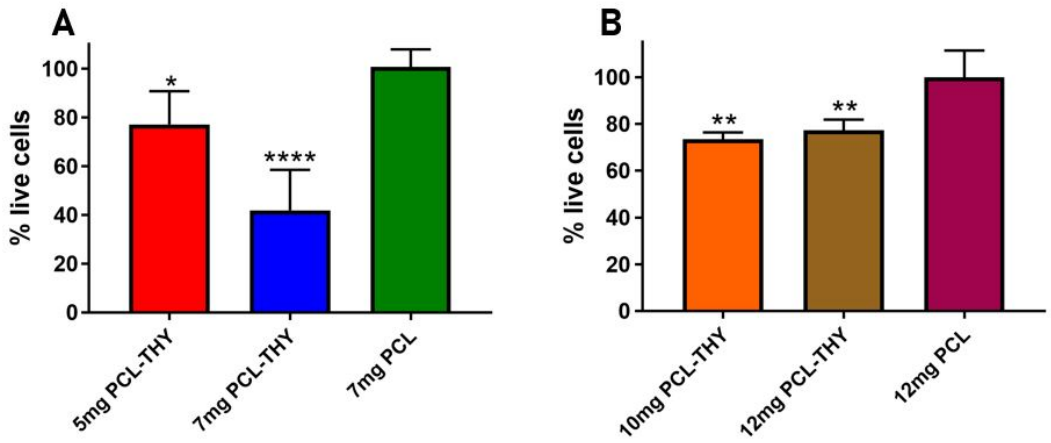

Figure 5. J774 macrophages viability after treatment with PCL-THY following two different approaches regarding the patch weight and incubation times in accordance with the bactericidal effects and cell viability percentages obtained: (A) Treatment for 24h (5 and 7 mg of PCL-THY); (B) Treatment for 1h and incubation for other 24h (10 and 12 mg PCL-THY). The results are graphed in basis to untreated cells which were assigned with a 100% viability. *$p<0.05$; **$p<0.01$; ****$p<0.0001$. Mean ± SD of three replicas are represented.

3.5. *In vitro* model of infection of J774 macrophages

We previously visualized the effect of PCL-THY on bacteria growth and biofilm formation. As we mentioned before, macrophages play a crucial role in wound healing, managing pathogens, phagocytizing dead cells and recruiting other cells which help to fight infection, such as neutrophils, fibroblasts, keratinocytes or endothelial cells.[38,39] To investigate the

impact of the treatment of PCL-THY on a *S. aureus* infected cell line, J774 macrophages were visualized in contact with GFP-expressing *S. aureus*. Figures 6 and 7 represent the orthogonal projection using the maximum intensity projection (MIP), to visualize bacteria inside and outside cells, represented both in the same plane. Bacteria are shown in green while cell nuclei are stained with DAPI (blue) and cytoskeleton, with phalloidin 546 (red). Figure 6 depicts activated macrophages with LPS and treated with 5 and 7 mg of PCL-THY for 24h. Control samples (Figures 6A and 6B) showed cells totally filled with bacteria (green), indicating the successful infection of macrophages. However, the treatment with 5 mg of PCL-THY (Figures 6C and 6D) and 7 mg of PCL-THY (Figures 6E and 6F) for 24h clearly demonstrated the efficiency of the synthesized loaded antimicrobial patches showing a reduced number of bacteria in a dose-dependent manner. In the time span studied, 5 and 7 mg patches would release in 24h an amount of THY of 0.06 mg/mL and 0.09 mg/mL to the medium, respectively, concentration with which bacterial inhibition was detected.

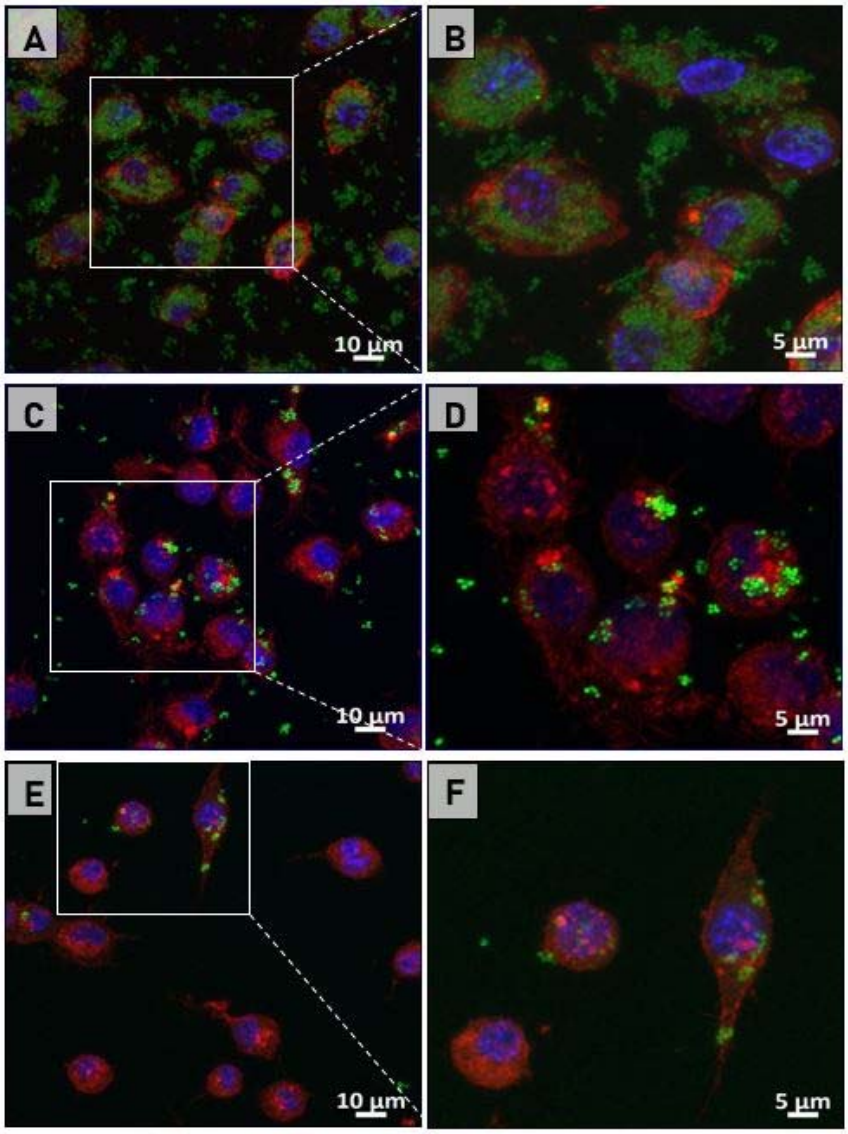

Figure 6. *In vitro* co-culture model of GFP-expressing *S. aureus* and J774 macrophages. Cells were treated for 24h with: (A, B) 7 mg of PCL patches (control samples); (C, D) 5 mg PCL-THY; (E, F) 7 mg PCL-THY. Left images were acquired with a 63x oil immersion objective. Right images correspond with a zoomed area of left images. Bacteria are stained in green while cell nuclei are stained with DAPI (blue) and cytoskeleton with phalloidin 546 (red).

524 Due to the results obtained in the cell toxicity study, infected macrophages were also treated
525 with 10 and 12 mg PCL-THY though reducing the incubation time to 1h (Figure 7). These
526 images demonstrated the same trend observed in the previous assay. When cells were treated
527 with 12 mg of THY-free PCL (Figures 7A and 7B), bacteria were found throughout the plate.
528 However, when cells were treated with 10 mg PCL-THY (0.12 mg/mL of THY released in
529 1h; Figures 7C and 7D) and 12 mg PCL-THY (0.14 mg/mL of THY released in 1h; Figures
530 7E and 7F) for 1h, bacteria concentration was significantly reduced, even totally when using
531 the highest amount, confirming the efficiency of the fabricated PCL-THY mats in an *in vitro*
532 infection model, pointing to their potential antibacterial application.
533

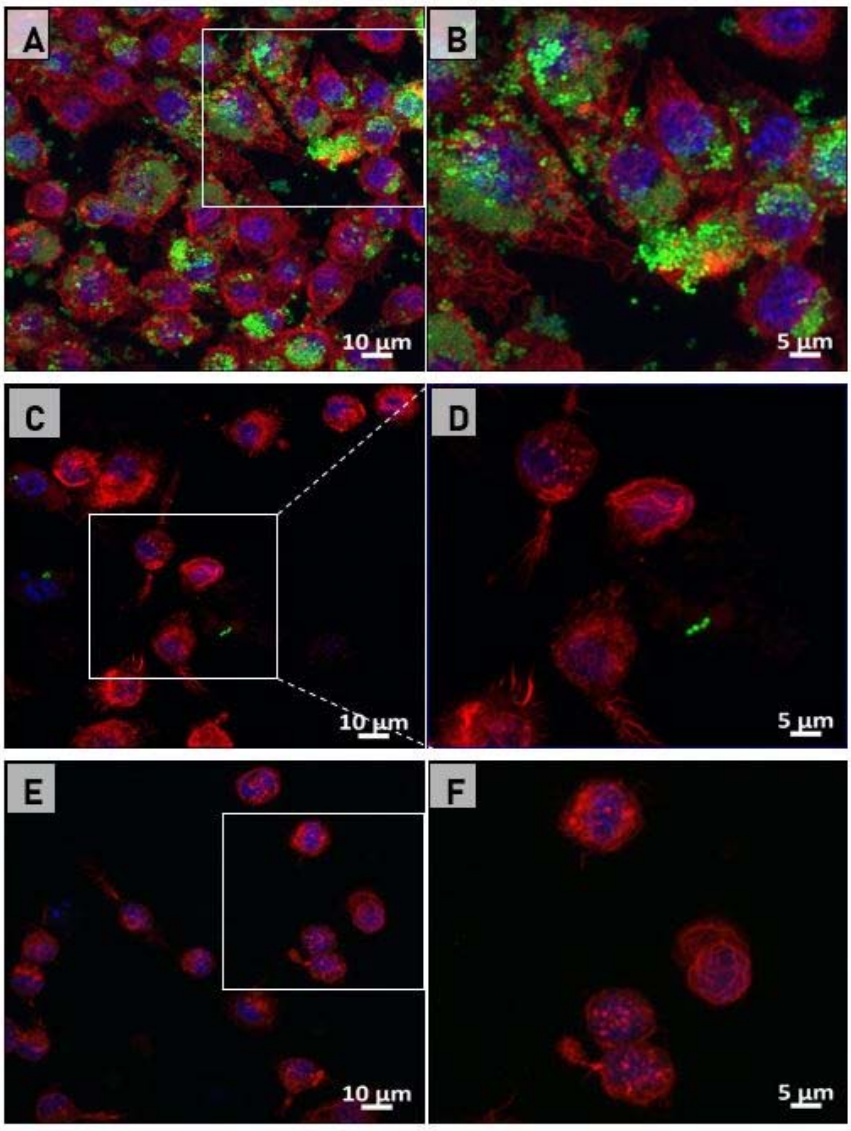

Figure 7. *In vitro* co-culture model of GFP-expressing *S. aureus* and J774 macrophages. Cells were treated for 24h with: (A, B) 12 mg of THY-free PCL; (C, D) 10 mg of PCL-THY; (E, F) 12 mg of PCL-THY. Left images were acquired with a 63x oil immersion objective. Right images correspond to a zoomed area of left images. Bacteria are stained in green while cell nuclei are stained with DAPI (blue) and cytoskeleton with phalloidin 546 (red).

Among other functions, biofilm allows bacteria to defense itself from external threats. Thus, immune cells are not able to reach and eliminate bacteria, and therefore a persistent inflammation and wound chronification occur.[58] *S. aureus* may survive within phagocytic cells including macrophages, even when the host defense is activated.[59] Based on that, GFP-expressing *S. aureus* was chosen as a model of a bacterial pathogen with part of its life cycle occurring intracellularly to study and visualize the effect of PCL-THY on J774 macrophages in a co-culture infection model. The treatment of GFP-expressing *S. aureus* for 24h with a sub-inhibitory concentration (7 mg of PCL-THY, 0.09 mg/mL THY released) was found as cytotoxic to macrophages. It is not the first time that a high toxicity of THY is reported in eukaryotic cell cultures. For example, Belato et al. analyzed the cytotoxicity of free THY on murine macrophages (RAW 264.7) and showed that cell viability dropped from 75% to 5% at concentrations higher than 0.005 mg/mL.[60] Prior studies of our group revealed a similar toxicity, obtaining a viability of 60% when J774 macrophages were treated with 0.12 mg/mL of free THY.[61] The toxicity mechanism of this compound is poorly understood. There are different hypothesis about this issue; Gutierrez et al. reported that THY can affect the integrity of membranes in both prokaryotic and eukaryotic cells.[62] However, Satooka *et al.* proposed that THY is intracellular transformed to a toxic radical and quinone, relating its toxicity to the oxidative-stress generated.[63]

Compared with bactericidal planktonic studies, when J774 macrophages were infected with GFP-expressing *S. aureus*, it has been shown that a lower dose of PCL-THY patches is able to fight cell infection. That is probably because THY may help macrophages to control the progression of the infection *in vitro*.[64] In summary, PCL-THY patches have demonstrated to induce a significant reduction of GFP-expressing *S. aureus* into infected J774 macrophages, diminishing their intracellular colonization. In addition, the ability of THY to reduce biofilm

582 formation, opens the possibility to fight bacterial infections and make the recovery of wound
583 healing more efficient when using this locally delivery system based on thymol.
584
585 ## 4. CONCLUSIONS
586 By comparing THY-free PCL electrospun patches as a model of a conventional wound
587 dressing and THY-eluting PCL electrospun patches, the later outstand as efficient
588 antimicrobial materials against pathogenic Gram-positive bacteria sensitive strains to
589 conventional antibiotics (ATCC 25923 strain, MSSA Newman strain expressing cGFP,
590 MSSA clinical strain), and in a lower extent to the MRSA clinical strain USA300. Moreover,
591 a fluorescent bacteria was also used to demonstrate the successful infective action of the
592 pathogen in eukaryotic cells as a model of intracellular pathogen. The developed advanced
593 wound dressings were also efficient in eradicating intracellular bacteria. Finally, we have
594 also demonstrated that the PCL-THY patches were able to remove already formed bacterial
595 biofilms and also inhibit the first stages of bacterial adhesion and biofilm formation in the
596 ATCC 25923 and cGFP strains, while the clinical strains biofilms (MSSA Newman and
597 MRSA USA300) were inhibited at the highest PCL-THY amounts assayed (30 mg). The
598 developed patches showed cytotoxicity against eukaryotic cells in a dose dependent manner,
599 but at reduced doses and during short contact times, cell viability was similar to that retrieved
600 for untreated controls. In this comparative study, research based on evidence demonstrated
601 that THY-loaded electrospun PCL patches are more efficient that their THY-free
602 counterparts against pathogenic *S. aureus*.
603
604 ## AUTHOR INFORMATION
605 ### Corresponding Authors

* (S.G-S) saragarciasalinas@gmail.com, (S.I.) sirusta@unizar.es, Tel.: +34 876555437.

Author Contributions

The manuscript was written through the contributions of all authors. All authors have given approval to the final version of the manuscript.

Notes

The authors declare no competing financial interest.

ACKNOWLEDGMENTS

This research was funded by the Spanish Ministry of Economy and Competitiveness (grant number grant number CTQ2017-84473-R). CIBER-BBN is an initiative funded by the VI National R&D&i Plan 2008–2011, Iniciativa Ingenio 2010, Consolider Program, CIBER Actions and financed by the Instituto de Salud Carlos III (Spain) with assistance from the European Regional Development Fund. The authors acknowledge the LMA/INA, the Cell Culture, and Microscopy Core Units from IACS/IIS Aragon for their instruments and expertise. S.G-S. gratefully acknowledges the support from the FPI program granted by the Spanish Ministry of Science, Innovation and Universities (BES-2015-073735). G.M. acknowledges the support from the Miguel Servet Program (MS19/00092; Instituto de Salud Carlos III).

REFERENCES

(1) Spellberg, B.; Gilbert, D. N. The Future of Antibiotics and Resistance: A Tribute to a Career of Leadership by John Bartlett. *Clin. Infect. Dis.* **2014**, *59* (Suppl 2), S71–S75. https://doi.org/10.1093/cid/ciu392.

(2) Bartlett, J. G.; Gilbert, D. N.; Spellberg, B. Seven Ways to Preserve the Miracle of Antibiotics. *Clin. Infect. Dis.* **2013**, *56* (10), 1445–1450.

https://doi.org/10.1093/cid/cit070.

(3) The Antibiotic Alarm. *Nature* **2013**, *495* (7440), 141. https://doi.org/10.1038/495141a.

(4) Golkar, Z.; Bagasra, O.; Gene Pace, D. Bacteriophage Therapy: A Potential Solution for the Antibiotic Resistance Crisis. *J. Infect. Dev. Ctries.* **2014**, *8* (2), 129–136. https://doi.org/10.3855/jidc.3573.

(5) Luyt, C. E.; Bréchot, N.; Trouillet, J. L.; Chastre, J. Antibiotic Stewardship in the Intensive Care Unit. *Crit. Care* **2014**, *18* (5), 1–12. https://doi.org/10.1186/s13054-014-0480-6.

(6) Bush, K.; Courvalin, P.; Dantas, G.; Davies, J.; Eisenstein, B.; Huovinen, P.; Jacoby, G. A.; Kishony, R.; Kreiswirth, B. N.; Kutter, E.; et al. Tackling Antibiotic Resistance. *Nat. Rev. Microbiol.* **2011**, *9* (12), 894–896. https://doi.org/10.1038/nrmicro2693.

(7) Klein, E. Y.; Van Boeckel, T. P.; Martinez, E. M.; Pant, S.; Gandra, S.; Levin, S. A.; Goossens, H.; Laxminarayan, R. Global Increase and Geographic Convergence in Antibiotic Consumption between 2000 and 2015. *Proc. Natl. Acad. Sci. U. S. A.* **2018**, *115* (15), E3463–E3470. https://doi.org/10.1073/pnas.1717295115.

(8) Scandorieiro, S.; de Camargo, L. C.; Lancheros, C. A. C.; Yamada-Ogatta, S. F.; Nakamura, C. V.; de Oliveira, A. G.; Andrade, C. G. T. J.; Duran, N.; Nakazato, G.; Kobayashi, R. K. T. Synergistic and Additive Effect of Oregano Essential Oil and Biological Silver Nanoparticles against Multidrug-Resistant Bacterial Strains. *Front. Microbiol.* **2016**, *7* (MAY), 1–14. https://doi.org/10.3389/fmicb.2016.00760.

(9) Becerril, R.; Nerín, C.; Gómez-Lus, R. Evaluation of Bacterial Resistance to Essential Oils and Antibiotics after Exposure to Oregano and Cinnamon Essential

Oils. *Foodborne Pathog. Dis.* **2012**, *9* (8), 699–705. https://doi.org/10.1089/fpd.2011.1097.

(10) Di Pasqua, R.; Hoskins, N.; Betts, G.; Mauriello, G. Changes in Membrane Fatty Acids Composition of Microbial Cells Induced by Addiction of Thymol, Carvacrol, Limonene, Cinnamaldehyde, and Eugenol in the Growing Media. *J. Agric. Food Chem.* **2006**, *54* (7), 2745–2749. https://doi.org/10.1021/jf052722l.

(11) Deb, D. D.; Parimala, G.; Saravana Devi, S.; Chakraborty, T. Effect of Thymol on Peripheral Blood Mononuclear Cell PBMC and Acute Promyelotic Cancer Cell Line HL-60. *Chem. Biol. Interact.* **2011**, *193* (1), 97–106. https://doi.org/10.1016/j.cbi.2011.05.009.

(12) García-Salinas, S.; Elizondo-Castillo, H.; Arruebo, M.; Mendoza, G.; Irusta, S. Evaluation of the Antimicrobial Activity and Cytotoxicity of Different Components of Natural Origin Present in Essential Oils. *Molecules* **2018**, *23* (6), 1–18. https://doi.org/10.3390/molecules23061399.

(13) Gresham, H. D.; Lowrance, J. H.; Caver, T. E.; Wilson, B. S.; Cheung, A. L.; Lindberg, F. P. Survival of Staphylococcus Aureus Inside Neutrophils Contributes to Infection . *J. Immunol.* **2000**, *164* (7), 3713–3722. https://doi.org/10.4049/jimmunol.164.7.3713.

(14) Froiio, F.; Ginot, L.; Paolino, D.; Lebaz, N.; Bentaher, A.; Fessi, H.; Elaissari, A. Essential Oils-Loaded Polymer Particles: Preparation, Characterization and Antimicrobial Property. *Polymers (Basel).* **2019**, *11* (6). https://doi.org/10.3390/polym11061017.

(15) Hamed Laroui, Poonam Rakhya, Bo Xiao, E. V. and D. M. Nanotechnology in Diagnostics and Therapeutics for Gastrointestinal Disorders. *Bone* **2013**, *45* (12),

995–1002. https://doi.org/10.1038/jid.2014.371.

(16) Sill, T. J.; von Recum, H. A. Electrospinning: Applications in Drug Delivery and Tissue Engineering. *Biomaterials* **2008**, *29* (13), 1989–2006. https://doi.org/10.1016/j.biomaterials.2008.01.011.

(17) Gilchrist, S. E.; Lange, D.; Letchford, K.; Bach, H.; Fazli, L.; Burt, H. M. Fusidic Acid and Rifampicin Co-Loaded PLGA Nanofibers for the Prevention of Orthopedic Implant Associated Infections. *J. Control. Release* **2013**, *170* (1), 64–73. https://doi.org/10.1016/j.jconrel.2013.04.012.

(18) Manesh, K. M.; Santhosh, P.; Gopalan, A.; Lee, K. P. Electrospun Poly(Vinylidene Fluoride)/Poly(Aminophenylboronic Acid) Composite Nanofibrous Membrane as a Novel Glucose Sensor. *Anal. Biochem.* **2007**, *360* (2), 189–195. https://doi.org/10.1016/j.ab.2006.09.021.

(19) Gámez, E.; Mendoza, G.; Salido, S.; Arruebo, M.; Irusta, S. Antimicrobial Electrospun Polycaprolactone-Based Wound Dressings: An in Vitro Study about the Importance of the Direct Contact to Elicit Bactericidal Activity. *Adv. Wound Care* **2019**, *8* (9), 438–451. https://doi.org/10.1089/wound.2018.0893.

(20) Rasouli, R.; Barhoum, A.; Bechelany, M.; Dufresne, A. Nanofibers for Biomedical and Healthcare Applications. *Macromol. Biosci.* **2019**, *19* (2), 1–27. https://doi.org/10.1002/mabi.201800256.

(21) Zeng, H.; Cui, J.; Cao, B.; Gibson, U.; Bando, Y.; Golberg, D. Electrochemical Deposition of ZnO Nanowire Arrays: Organization, Doping and Properties. *Sci. Adv. Mater.* **2010**, *2* (3), 336–358.

(22) Jiang, S.; Chen, Y.; Duan, G.; Mei, C.; Greiner, A.; Agarwal, S. Electrospun Nanofiber Reinforced Composites: A Review. *Polym. Chem.* **2018**, *9* (20), 2685–

2720. https://doi.org/10.1039/c8py00378e.

(23) Jang, C. H.; Cho, Y. B.; Jang, Y. S.; Kim, M. S.; Kim, G. H. Antibacterial Effect of Electrospun Polycaprolactone/Polyethylene Oxide/Vancomycin Nanofiber Mat for Prevention of Periprosthetic Infection and Biofilm Formation. *Int. J. Pediatr. Otorhinolaryngol.* **2015**, *79* (8), 1299–1305. https://doi.org/10.1016/j.ijporl.2015.05.037.

(24) Guarino, V.; Cruz-Maya, I.; Altobelli, R.; Abdul Khodir, W. K.; Ambrosio, L.; Alvarez Pèrez, M. A.; Flores, A. A. Electrospun Polycaprolactone Nanofibres Decorated by Drug Loaded Chitosan Nano-Reservoirs for Antibacterial Treatments. *Nanotechnology* **2017**, *28* (50). https://doi.org/10.1088/1361-6528/aa9542.

(25) Adeli-sardou, M.; Torkzadeh-Mahani, M.; Yaghoobi, M. M.; Dodel, M. Antibacterial and Anti-Biofilm Investigation of Electrospun PCL/Gelatin/Lawsone Nano Fiber Scaffolds against Biofilm Producing Bacteria. *Biomacromolecular J.* **2018**, *4* (1), 46–57.

(26) Costerton, J. W.; Stewart, P. S.; Greenberg, E. P. Bacterial Biofilms: A Common Cause of Persistent Infections. *Science (80-.).* **1999**, *284* (5418), 1318–1322. https://doi.org/10.1126/science.284.5418.1318.

(27) Bassler, B. L.; Losick, R. Bacterially Speaking. *Cell* **2006**, *125* (2), 237–246. https://doi.org/10.1016/j.cell.2006.04.001.

(28) Hall-Stoodley, L.; Costerton, J. W.; Stoodley, P. Bacterial Biofilms: From the Natural Environment to Infectious Diseases. *Nat. Rev. Microbiol.* **2004**, *2* (2), 95–108. https://doi.org/10.1038/nrmicro821.

(29) Kerekes, E. B.; Vidács, A.; Takó, M.; Petkovits, T.; Vágvölgyi, C.; Horváth, G.; Balázs, V. L.; Krisch, J. Anti-Biofilm Effect of Selected Essential Oils and Main

Components on Mono- and Polymicrobic Bacterial Cultures. *Microorganisms* **2019**, *7* (9). https://doi.org/10.3390/microorganisms7090345.

(30) Quave, C. L.; Estévez-Carmona, M.; Compadre, C. M.; Hobby, G.; Hendrickson, H.; Beenken, K. E.; Smeltzer, M. S. Ellagic Acid Derivatives from Rubus Ulmifolius Inhibit Staphylococcus Aureus Biofilm Formation and Improve Response to Antibiotics. *PLoS One* **2012**, *7* (1). https://doi.org/10.1371/journal.pone.0028737.

(31) Sharifi, A.; Mohammadzadeh, A.; Zahraei Salehi, T.; Mahmoodi, P. Antibacterial, Antibiofilm and Antiquorum Sensing Effects of Thymus Daenensis and Satureja Hortensis Essential Oils against Staphylococcus Aureus Isolates. *J. Appl. Microbiol.* **2018**, *124* (2), 379–388. https://doi.org/10.1111/jam.13639.

(32) Čabarkapa, I.; Čolović, R.; Đuragić, O.; Popović, S.; Kokić, B.; Milanov, D.; Pezo, L. Anti-Biofilm Activities of Essential Oils Rich in Carvacrol and Thymol against Salmonella Enteritidis. *Biofouling* **2019**, *35* (3), 361–375. https://doi.org/10.1080/08927014.2019.1610169.

(33) Duerden, B. I. Virulence Factors in Anaerobes. *Clin. Infect. Dis.* **1994**, *18*, S253–S259. https://doi.org/10.1093/clinids/18.Supplement_4.S253.

(34) Malone, M.; Bjarnsholt, T.; McBain, A. J.; James, G. A.; Stoodley, P.; Leaper, D.; Tachi, M.; Schultz, G.; Swanson, T.; Wolcott, R. D. The Prevalence of Biofilms in Chronic Wounds: A Systematic Review and Meta-Analysis of Published Data. *J. Wound Care* **2017**, *26* (1), 20–25. https://doi.org/10.12968/jowc.2017.26.1.20.

(35) Moyano, A. J.; Mas, C. R.; Colque, C. A.; Smania, A. M. Dealing with Biofilms of Pseudomonas Aeruginosa and Staphylococcus Aureus: In Vitro Evaluation of a Novel Aerosol Formulation of Silver Sulfadiazine. *Burns* **2019**, *46* (1), 128–135. https://doi.org/10.1016/j.burns.2019.07.027.

(36) Johnson, J. T.; Yu, V. L. Role of Anaerobic Bacteria in Postoperative Wound Infections Following Oncologic Surgery of the Head and Neck. *Ann. Otol. Rhinol. Laryngol.* **1991**, *100* (9 II SUPPL. 154), 46–48. https://doi.org/10.1177/00034894911000s913.

(37) Cutting, K. F.; White, R. J. Criteria for Identifying Wound Infection--Revisited. *Ostomy. Wound. Manage.* **2005**, *51* (1), 28–34.

(38) Martin, P.; Leibovich, S. J. Inflammatory Cells during Wound Repair: The Good, the Bad and the Ugly. *Trends Cell Biol.* **2005**, *15* (11), 599–607. https://doi.org/10.1016/j.tcb.2005.09.002.

(39) Krzyszczyk, P.; Schloss, R.; Palmer, A.; Berthiaume, F. The Role of Macrophages in Acute and Chronic Wound Healing and Interventions to Promote Pro-Wound Healing Phenotypes. *Front. Physiol.* **2018**, *9* (MAY), 1–22. https://doi.org/10.3389/fphys.2018.00419.

(40) Mal, P.; Dutta, K.; Bandyopadhyay, D.; Basu, A.; Khan, R.; Bishayi, B. Azithromycin in Combination with Riboflavin Decreases the Severity of Staphylococcus Aureus Infection Induced Septic Arthritis by Modulating the Production of Free Radicals and Endogenous Cytokines. *Inflamm. Res.* **2013**, *62* (3), 259–273. https://doi.org/10.1007/s00011-012-0574-z.

(41) Miramoth, N. S.; Di Meo, C.; Zouhiri, F.; Saïd-Hassane, F.; Valetti, S.; Gorges, R.; Nicolas, V.; Poupaert, J. H.; Chollet-Martin, S.; Desmaële, D.; et al. Self-Assembled Squalenoylated Penicillin Bioconjugates: An Original Approach for the Treatment of Intracellular Infections. *ACS Nano* **2012**, *6* (5), 3820–3831. https://doi.org/10.1021/nn204928v.

(42) Dey, S.; Bishayi, B. Killing of Staphylococcus Aureus in Murine Macrophages by

Chloroquine Used Alone and in Combination with Ciprofloxacin or Azithromycin. *J. Inflamm. Res.* **2015**, *8*, 29–47. https://doi.org/10.2147/JIR.S76045.

(43) Mendoza, G.; Regiel-Futyra, A.; Andreu, V.; Sebastián, V.; Kyzioł, A.; Stochel, G.; Arruebo, M. Bactericidal Effect of Gold-Chitosan Nanocomposites in Coculture Models of Pathogenic Bacteria and Human Macrophages. *ACS Appl. Mater. Interfaces* **2017**, *9* (21), 17693–17701. https://doi.org/10.1021/acsami.6b15123.

(44) Patel J.B., Cockerill R.F., Bradford A.P., Eliopoulos M.G., Hindler A.J., Jenkins G.S., Lewis S.J., Limbago B., Miller A.L., Nicolau P.D., Pwell M., Swenson M.J., Traczewski M.M., Turnidge J.D., W. P. M. Z. L. B. M07-A10: Methods for Dilution Antimicrobial Susceptibility Tests for Bacteria That Grow Aerobically; Approved Standard—Tenth Edition. *CLSI (Clinical Lab. Stand. Institute)* **2015**, *35* (2). https://doi.org/10.1007/s00259-009-1334-3.

(45) International, A. *ASTM E2180-18, Standard Test Method for Determining the Activity of Incorporated Antimicrobial Agent(s) In Polymeric or Hydrophobic Materials*; West Conshohecken, PA, 2018.

(46) Sadeghianmaryan, A.; Yazdanpanah, Z.; Soltani, Y. A.; Sardroud, H. A.; Nasirtabrizi, M. H.; Chen, X. Curcumin-loaded Electrospun Polycaprolactone/Montmorillonite Nanocomposite: Wound Dressing Application with Anti-bacterial and Low Cell Toxicity Properties. *J. Biomater. Sci. Polym. Ed.* **2019**, *0* (0), 000. https://doi.org/10.1080/09205063.2019.1680928.

(47) Alves, P. E.; Soares, B. G.; Lins, L. C.; Livi, S.; Santos, E. P. Controlled Delivery of Dexamethasone and Betamethasone from PLA Electrospun Fibers: A Comparative Study. *Eur. Polym. J.* **2019**, *117* (April), 1–9. https://doi.org/10.1016/j.eurpolymj.2019.05.001.

(48) Alfaro De Prá, M. A.; Ribeiro-do-Valle, R. M.; Maraschin, M.; Veleirinho, B. Effect of Collector Design on the Morphological Properties of Polycaprolactone Electrospun Fibers. *Mater. Lett.* **2017**, *193*, 154–157. https://doi.org/10.1016/j.matlet.2017.01.102.

(49) Aragón, J.; Costa, C.; Coelhoso, I.; Mendoza, G.; Aguiar-Ricardo, A.; Irusta, S. Electrospun Asymmetric Membranes for Wound Dressing Applications. *Mater. Sci. Eng. C* **2019**, *103* (April), 109822. https://doi.org/10.1016/j.msec.2019.109822.

(50) Peppas, N. A.; Sahlin, J. J. A Simple Equation for the Description of Solute Release. III. Coupling of Diffusion and Relaxation. *Int. J. Pharm.* **1989**, *57* (2), 169–172. https://doi.org/10.1016/0378-5173(89)90306-2.

(51) Badawy, M. E. I.; Marei, G. I. K.; Rabea, E. I.; Taktak, N. E. M. Antimicrobial and Antioxidant Activities of Hydrocarbon and Oxygenated Monoterpenes against Some Foodborne Pathogens through in Vitro and in Silico Studies. *Pestic. Biochem. Physiol.* **2019**, *158* (May), 185–200. https://doi.org/10.1016/j.pestbp.2019.05.008.

(52) Rúa, J.; Del Valle, P.; De Arriaga, D.; Fernández-Álvarez, L.; García-Armesto, M. R. Combination of Carvacrol and Thymol: Antimicrobial Activity Against Staphylococcus Aureus and Antioxidant Activity. *Foodborne Pathog. Dis.* **2019**, *16* (9), 622–629. https://doi.org/10.1089/fpd.2018.2594.

(53) Leaper, D. J.; Schultz, G.; Carville, K.; Fletcher, J.; Swanson, T.; Drake, R. Extending the TIME Concept: What Have We Learned in the Past 10 Years? *Int. Wound J.* **2012**, *9* (Suppl 2), 1–19.

(54) Yuan, Z.; Dai, Y.; Ouyang, P.; Rehman, T.; Hussain, S.; Zhang, T.; Yin, Z.; Fu, H.; Lin, J.; He, C.; et al. Thymol Inhibits Biofilm Formation, Eliminates Pre- Existing Biofilms, and Enhances Clearance of Methicillin-resistant Staphylococcus Aureus

(MRSA) in a Mouse Peritoneal Implant Infection Model. *Microorganisms* **2020**, *8* (1), 1–17. https://doi.org/10.3390/microorganisms8010099.

(55) Chung, P. Y.; Toh, Y. S. Anti-Biofilm Agents: Recent Breakthrough against Multi-Drug Resistant Staphylococcus Aureus. *Pathog. Dis.* **2014**, *70* (3), 231–239. https://doi.org/10.1111/2049-632X.12141.

(56) Joo, H. S.; Otto, M. Molecular Basis of in Vivo Biofilm Formation by Bacterial Pathogens. *Chem. Biol.* **2012**, *19* (12), 1503–1513. https://doi.org/10.1016/j.chembiol.2012.10.022.

(57) *ISO 10993-5:2009—Biological Evaluation of Medical Devices—Part 5: Tests for In Vitro Cytotoxicity.*; 2009.

(58) Wolcott, R.; Dowd, S. The Role of Biofilms: Are We Hitting the Right Target? *Plast. Reconstr. Surg.* **2011**, *127* (SUPPL. 1 S), 28–35. https://doi.org/10.1097/PRS.0b013e3181fca244.

(59) Underhill, D. M.; Goodridge, H. S. Information Processing during Phagocytosis. *Nat. Rev. Immunol.* **2012**, *12* (7), 492–502. https://doi.org/10.1038/nri3244.

(60) Belato, K. K.; de Oliveira, J. R.; de Oliveira, F. S.; de Oliveira, L. D.; Camargo, S. E. A. Cytotoxicity and Genotoxicity of Thymol Verified in Murine Macrophages (RAW 264.7) after Antimicrobial Analysis in Candida Albicans, Staphylococcus Aureus, and Streptococcus Mutans. *J. Funct. Foods* **2018**, *40* (August 2017), 455–460. https://doi.org/10.1016/j.jff.2017.11.035.

(61) García-Salinas, S.; Evangelopoulos, M.; Gámez-Herrera, E.; Arruebo, M.; Irusta, S.; Taraballi, F.; Mendoza, G.; Tasciotti, E. Electrospun Anti-Inflammatory Patch Loaded with Essential Oils for Wound Healing. *Int. J. Pharm.* **2020**, *577*, 119067. https://doi.org/10.1016/j.ijpharm.2020.119067.

(62) Gutiérrez, L.; Batlle, R.; Sánchez, C.; Nerín, C. New Approach to Study the Mechanism of Antimicrobial Protection of an Active Packaging. *Foodborne Pathog. Dis.* **2010**, *7* (9), 1063–1069. https://doi.org/10.1089/fpd.2009.0516.

(63) Satooka, H.; Kubo, I. Effects of Thymol on B16-F10 Melanoma Cells. *J. Agric. Food Chem.* **2012**, *60* (10), 2746–2752. https://doi.org/10.1021/jf204525b.

(64) Oliveira, J. R. de; de Jesus Viegas, D.; Martins, A. P. R.; Carvalho, C. A. T.; Soares, C. P.; Camargo, S. E. A.; Jorge, A. O. C.; de Oliveira, L. D. Thymus Vulgaris L. Extract Has Antimicrobial and Anti-Inflammatory Effects in the Absence of Cytotoxicity and Genotoxicity. *Arch. Oral Biol.* **2017**, *82* (June), 271–279. https://doi.org/10.1016/j.archoralbio.2017.06.031.